

# The Rate-Controlling Substrate of Nitrilotriacetate for Biodegradation by *Chelatobacter heintzii*

J. M. VANBRIESEN,<sup>\*,†</sup> B. E. RITTMANN,<sup>†</sup>  
L. XUN,<sup>‡</sup> D. C. GIRVIN,<sup>§</sup> AND  
H. BOLTON, JR.<sup>#</sup>

Department of Civil Engineering, Northwestern University,  
2145 Sheridan Road, Evanston, Illinois 60208-3109,  
Microbiology Department, Washington State University, 387  
Eastlick, Pullman, Washington 99164-4233, and Interfacial  
Geochemistry and Environmental Microbiology Groups,  
Pacific Northwest National Laboratory, 902 Battelle  
Boulevard, Richland, Washington 99352

Codisposal of anthropogenic chelating agents such as nitrilotriacetate (NTA) with radioactive and heavy metals can enhance environmental transport of the metals, extending subsurface contamination and threatening groundwater sources. The biodegradation of the chelating agent can lead to the immobilization of the chelated metal and radionuclide contaminants. The rate of biodegradation of the organic complexing agent may depend on the concentration of a specific, biologically available form of the chelate. In mixtures of metals and chelating agents, the relative distribution of different chemical forms of the chelate at equilibrium is controlled by the total concentrations of organic and inorganic constituents and thermodynamic stability constants for the aqueous complexes that form. In this paper, we evaluate experimental results for biodegradation of NTA by *Chelatobacter heintzii* in different metal/NTA systems in order to identify the chelate form controlling the rate of degradation. The  $\text{CaNTA}^-$  is the only species that can control the rate of NTA degradation in our systems. Our analysis of the potentially rate-limiting reactions in the biodegradation of NTA indicates that kinetically controlled complexation in the NTA system is not affecting the biodegradation of the chelate. The rate of transport of  $\text{CaNTA}^-$  into the cell appears to control the overall rate of NTA degradation. Thus, we expect enhanced rates of biological degradation of the chelate and immobilization of codisposed metals when  $\text{CaNTA}^-$  is available to *C. heintzii*.

## Introduction

Nitrilotriacetate (NTA) is an anthropogenic chelating agent widely used in nuclear waste processing and reactor decontamination (1–3). Codisposal of chelating agents and radioactive and heavy metals can lead to enhanced transport

of the metals away from disposal sites due to the increased solubility of metal-chelate complexes compared to uncomplexed metals (4). This transport extends subsurface contamination zones and can threaten metal and radionuclide contamination of groundwater. Biodegradation of the chelating agents releases the complexed metals and may reduce their mobility. The rate and extent of NTA biodegradation is affected by the kinetics of microbial utilization (5–8), the formation and utilization of intermediates (9–11), and the chemical form of the chelate available to the organisms (12–19). In previous work (20), we evaluated the importance of the formation of intermediates and the kinetics of each step in the degradation pathway. In the present paper, we evaluate the impact of the chelate speciation on the rate of NTA degradation.

The effect of chemical speciation on NTA degradation has been widely reported (12–19). However, many studies did not identify the microbiological species involved and the chemical environment in which degradation took place. In some cases, metal toxicity further complicated the relationship between aqueous speciation and biodegradation of NTA (14, 17).

Two previous studies have attempted to determine the effect of metal speciation on NTA degradation. Firestone and Tiedje (17) reported that a *Pseudomonas* species (ATCC 27109 and ATCC 29600, later reclassified as *Chelatobacter heintzii* (5)) degraded Ca, Mn, Mg, Fe, and Na chelates of NTA at nearly equal rates. Cu and Zn systems showed slower degradation, and Ni, Cd, and Hg systems showed no degradation. The experimental system utilized equimolar NTA/Me concentrations; however, this methodology did not always lead to the Me-NTA complex being the dominant aqueous form, thus complicating conclusions regarding the direct degradation of complexes. Also, metal toxicity effects were implicated in the slower degradation in the Cu, Zn, Ni, Cd, and Hg systems. Bolton et al. (21) report that *C. heintzii* degrades NTA in equimolar NTA/metal systems containing Co, Fe, Zn, Al, Cu, and Ni at different rates. Their experimental results are reviewed in the next section.

Initiating biodegradation requires at least two reactions that could depend on the chemical form of the substrate: transport of the substrate into the cell and reaction of the substrate with the enzyme that catalyzes the first step of degradation. If the transportable form is not dominant in the aqueous environment or is not the enzyme-active form, additional speciation exchange reactions, which usually are rapid, may be required. The potential rate-limiting reactions involved in NTA degradation by *C. heintzii* are as follows: (1) the rate of exchange of NTA species in solution outside the cell to the transportable NTA form, (2) the rate of transport of the transportable NTA form across the cell membrane by an unidentified NTA transport protein, (3) the rate of exchange of the transportable NTA form to the enzyme-active NTA form in the cell cytoplasm, (4) the rate of enzymatic activity on the enzyme-active NTA form, and (5) the rate of electron transfer from the enzyme-active NTA form to the electron acceptor,  $\text{O}_2$ .

For any of these five reactions, the rate could be controlled by the intrinsic kinetics of the step or by the effect of chemical speciation on the concentration of the relevant NTA form. We evaluate electron transport (point 5 above) first. McCarty (22) reports the maximum internal rate of electron flow from electron donor to electron acceptor,  $q_e$ , is between 1 and 2 electron equivalents per gram of volatile suspended solids (VSS) per day at 20 °C for many carbon-source electron-donor substrates. Assuming this value represents the rate of

\* Corresponding author phone: (412)268-4603; fax: (412)268-7813; e-mail: jeanne@cmu.edu. Current address: Department of Civil and Environmental Engineering, Carnegie Mellon University, Pittsburgh, PA 15213-3890.

† Northwestern University

‡ Washington State University.

§ Interfacial Geochemistry, Pacific Northwest National Laboratory.

# Environmental Microbiology Groups, Pacific Northwest National Laboratory.

electron transfer with no substrate-transport or exchange limitations,  $q_e$  can be used to estimate  $q_{\max}$ , the maximum specific rate of substrate utilization (22) for NTA degradation

$$q_{\max} = \frac{q_e \left( \frac{e^- \text{ eq donor}}{gVSS - \text{ day}} \right)}{f_e^o} \times \frac{\text{mol donor}}{n e^- \text{ eq donor}} \times \frac{\text{day}}{24 \text{ h}} \times \frac{113gVSS}{\text{mol cells}} \quad (1)$$

where  $f_e^o$  is the fraction of electrons from the donor sent to the acceptor for energy generation,  $n$  is the number of electron equivalents available per mol of the donor, and the molecular weight of cells is computed from an assumed cell composition of  $C_5H_7O_2N$  (22–30). For *C. heintzii*,  $f_e^o$  for NTA mineralization is approximately 0.3 (20, 31). Thus, the predicted maximum rate of substrate utilization for NTA is 3.3–6.6 mol substrate-mol cells<sup>-1</sup> h<sup>-1</sup>. However, the experimentally determined maximum rate of substrate utilization for NTA is 0.25–0.45 mol substrate-mol cells<sup>-1</sup> h<sup>-1</sup> (5, 6, 32, 33). This suggests electron transfer to the electron acceptor is not the rate-limiting step. Instead, the rate of degradation must be slowed prior to the electron-transfer step.

Next, we evaluate point 4, the reaction catalyzed by the NTA-degrading enzyme. The chemical form that is actively degraded by the enzyme depends on the bacterial species and degradation pathway. Several pathways for NTA degradation in key bacterial species have been elucidated (9–11, 16, 34, 35), and the first step of NTA degradation is carried out by a NTA-specific monooxygenase (NTA-MO) or a NTA-specific dehydrogenase (NTA-DH) (10). NTA-MO uses Mg<sup>2+</sup>-complexed NTA as its preferred substrate, but the Mg<sup>2+</sup> can be replaced by Mn<sup>2+</sup>, Ni<sup>2+</sup>, Co<sup>2+</sup>, or Fe<sup>2+</sup> (10, 11, 36). NTA-DH appears to utilize an uncomplexed, acid form of NTA, as no metal dependence has been observed (10, 37).

*C. heintzii* is an obligate aerobe, and NTA-MO catalyzes its first step in NTA degradation. The enzymatic activity of NTA-MO has been extensively researched (38). The  $K_m$  for NTA-MO in cell free extracts with Mg-NTA (its preferred substrate) is reported by Xun et al. (38) as 40 μM for MgNTA and by Egli (10) as 500 μM for MgNTA. However, in systems including cells, the Monod half-maximum rate constant,  $K_s$ , is reported as between 0.4 and 30 mM for total NTA (39). The Monod constants have been measured in activated sludge systems that may or may not contain *C. heintzii* as the dominant NTA degrading organism. Serological studies using indirect immunofluorescence testing (IFG) indicate *C. heintzii* or related organisms make up 0.1–1% of all organisms in sewage treatment plants (40). Rates of NTA consumption in activated sludge (39, 41) are similar to maximum rates reported for pure cultures of *C. heintzii* (41). While these studies suggest that kinetic parameters measured in activated sludge are suitable for modeling *C. heintzii*, they provide no additional insight into the potential for rate limitation via the enzyme step.

Reactions 1 and 3 refer to kinetics for exchange of NTA among aqueous forms. In general, aqueous speciation reactions are rapid and reach thermodynamic equilibrium quickly (42–44). In some rare cases, complexation-exchange kinetics affect speciation (45, 46). In general, therefore, we would not anticipate that these reactions limit the degradation rate of NTA. However, NTA biodegradation rate control by the relative rates of aqueous exchange in mixed metal/NTA systems was considered by Bolton et al. (19) who concluded that because different degradation rates were observed in different Me/NTA systems and the differences could not be explained by speciation effects on the concentration of the rate-controlling form, lability of the metal-NTA complex may have played a role in limiting the rate of

degradation. In their analysis, they assumed HNTA<sup>2-</sup> was the transported form and reviewed literature values for the exchange kinetics between the dominant aqueous metal-NTA complexes and the transportable HNTA<sup>2-</sup>. Their results suggest that nonlabile metal-NTA complexes may have limited the solution concentration of the transportable form and thus reduced the overall rate of NTA degradation in the system.

Limitation via step 2, the transport of NTA across the cell membrane, is the final possibility, and it has not been completely explored experimentally. Little is known about the uptake transport mechanism of NTA for any bacterial species. Wong et al. (47) reported a mutant that utilized an energy-dependent transport protein. Firestone and Tiedje (17) suggested that an NTA-binding protein for transport was likely, because the low Monod half-maximum rate constant ( $K_m < 10^{-4}$  M total NTA) indicated a high affinity for NTA. They suggested that the transportable form is an uncomplexed, acid form of NTA, because metals were not associated with the cells after degradation, and cells interrupted during degradation in a system with Fe-NTA as the dominant chemical form showed no excretion of Fe. Bolton et al. (19) also suggested that a specific transport protein may be involved in the *C. heintzii* system and recommended further studies with membrane vesicles to confirm this hypothesis. However, no specific NTA or Me-NTA transport protein has been isolated, and no direct evidence that transport depends on chelate speciation has been reported.

This initial analysis leads us to hypothesize that NTA degradation is probably controlled by the rate of transport of a specific, transportable NTA form into the cells (point 2 above), although limitation by the rate of exchange of metal-NTA forms outside the cell prior to transport or inside the cell prior to enzyme activity (points 1 and 3 above) is also possible. In this paper, we begin with a reanalysis of the data of Bolton et al. (19) utilizing a coupled biogeochemical model CCBATC to identify the rate-limiting step and the chemical form controlling this step for NTA degradation by *C. heintzii*. The reanalysis of these data suggest calcium plays a role in speciation-controlled degradation of NTA. We evaluated this with additional experimental work reported here for the first time.

## Materials and Methods

**Experimental Methods.** We use two distinct data sets and experimental investigations of NTA transport into whole cell. The two data sets have been previously reported, and the methods used in these studies are only summarized here (19, 48). The experimental investigation of NTA transport is new work completed to provide confirmation of model results of the earlier work. Data set one (19) had equimolar (to NTA) additions of Fe, Co, Mg, Ca, Ni, Zn, Al, or Cu, while data set two (48) had no added metals, but different fixed pH conditions. For data set one, *C. heintzii* was grown on plates, washed, and suspended in pH 6 buffer (0.001 M piperazine-N-N'-bis(2-ethanesulfonic acid) [PIPES] and 0.01 M KNO<sub>3</sub>). PIPES has a low complexing ability for a wide range of metals (49, 50) and does not compete with NTA for complexing the metals in solution. For data set two, cells were grown in suspended batch culture, centrifuged, washed, and suspended in pH buffer. In both experiments, cells were added at 10<sup>8</sup> colony forming units (CFU) mL<sup>-1</sup> (determined by serial dilution and plating onto NTA minimal medium). The NTA solution was present at a final NTA concentration of 5.23 and 1 micromolar for data sets one and two, respectively. NTA was uniformly labeled with C-14. During the degradation, serum bottles were destructively sampled by acidification and a CO<sub>2</sub> trap containing KOH was analyzed by carbon-14 liquid scintillation counting. Because metals released from the biomass may have contributed to the speciation of the

NTA, the contribution of metals from *C. heintzii* released into solution with the NTA was determined. *C. heintzii* was added at  $10^9$  CFU mL<sup>-1</sup> to pH 6 buffer containing 52 μM NTA. The cells were incubated and then centrifuged. The supernatant was filtered, acidified, and assayed for Al, Ca, Cd, Co, Cu, Fe, K, Mg, Mn, Na, Ni, and Zn by inductively coupled plasma-atom emission spectroscopy (19). The metal concentrations for the experimental conditions of  $10^8$  CFU mL<sup>-1</sup> and 5.23 μM NTA were assumed to be 10-fold less than observed in this manner and are reported by Bolton et al. (19).

**Metal Speciation Experiments.** The experiments in set one were designed to create different speciation based on the different metals added. Modeling with CCBATCH indicated that, in the absence of metals, the dominant form in solution was HNTA<sup>2-</sup>, while in the Me/NTA systems, the dominant NTA form in solution was a Me-NTA complex. In all cases, HNTA<sup>2-</sup> (the dominant acid form of NTA at the experimental conditions of pH 6) comprised between 2 and 99% of the NTA in solution, the uncomplexed NTA<sup>3-</sup> comprised between  $1 \times 10^{-6}$  and 0.1% of the total NTA, and CaNTA<sup>-</sup> comprised between  $9 \times 10^{-4}$  and 0.5% of the total NTA. The low metal concentrations were selected to ensure metal toxicity was not contributing to varying degradation rates, and the experimental system was designed with a high cell concentration, low NTA (substrate) concentration, and no growth nutrients in the experimental media to ensure similar cell densities for each experiment.

**Experimental Investigations of NTA Transport.** *C. heintzii* was grown with 5.23 mM NTA or 5 mM acetate in a defined liquid medium (19) at room temperature (22 °C) with shaking (150 rpms). Cells were harvested at mid-log phase by centrifugation at 8000g for 15 min and resuspended in pH 7 HEPES buffer [0.01 M N-(2-hydroxyethyl)piperazine-N'-ethanesulfonic acid (HEPES) adjusted to pH 7 with NH<sub>4</sub>-OH]. The HEPES buffer does not compete with NTA as a metal complexing agent (49). All transport experiments contained  $10^8$  CFU mL<sup>-1</sup>.

Cell suspension (1.4 mL) was added to triplicate 5-mL polypropylene test tubes. The assay was started by adding 0.1-mL of NTA solution as the cell suspension was vortexed. Samples (1-mL) were removed after 20 s and immediately filtered through a 0.2-μ filter under vacuum. The filter was washed with 5-mL of ice-cold buffer, and the filter was immediately placed into a scintillation vial containing cocktail, capped tightly, and shaken. The <sup>14</sup>C-labeled NTA (uniformly labeled-<sup>14</sup>C, 426 MBq mmol<sup>-1</sup>, 98% purity, Amersham, Arlington Heights, IL) was added with unlabeled compound and metals to provide the varying concentrations used in the assays. An assay time of 20 s was chosen because minimal <sup>14</sup>CO<sub>2</sub> was generation during this time period (e.g., 6% uptake and 0.045% <sup>14</sup>CO<sub>2</sub> generation). The cellular transport of CaNTA was investigated as discussed above using <sup>14</sup>C-NTA with unlabeled Ca and <sup>45</sup>Ca with unlabeled NTA. Assays included 1.5 micromolar NTA with Ca present at the following micromolar concentrations and the resulting micromolar concentration of CaNTA present in parentheses: 1 (0), 10 (0.25), 25 (0.50), 50 (0.75), 110 (1.00), 280 (1.25). Controls containing NTA or Ca only were subtracted from the treatments.

**Modeling Methods.** The NTA/*C. heintzii* system has been previously analyzed with the CCBATCH model (20, 30), and the stoichiometry and kinetic parameters for the stepwise degradation of NTA have been determined (20). CCBATCH is a coupled equilibrium-kinetic biogeochemical model designed to predict the behavior of complex chemical mixtures undergoing biological degradation in batch systems. Thermodynamic equilibrium is used to describe aqueous chemical reactions that take place in the bulk phase (acid/base and complexation) (42, 51–54), while kinetic repre-

sentations are used for interfacial reactions, including biological reactions.

The chemical components for the NTA-metal-*C. heintzii* system include NTA<sup>3-</sup> as the primary electron-donor substrate and carbon source, H<sup>+</sup>, H<sub>2</sub>CO<sub>3</sub>, NH<sub>4</sub><sup>+</sup>, O<sub>2</sub>, *C. heintzii* cells (represented as C<sub>5</sub>H<sub>7</sub>O<sub>2</sub>N (55)), soluble microbial products (SMP represented as C<sub>5</sub>H<sub>7</sub>O<sub>2</sub>N<sub>soluble</sub>), Al<sup>3+</sup>, Ca<sup>2+</sup>, Cd<sup>2+</sup>, Co<sup>2+</sup>, Cu<sup>2+</sup>, Fe<sup>3+</sup>, Mg<sup>2+</sup>, Ni<sup>2+</sup>, and Zn<sup>2+</sup>. The degradation intermediates, iminodiacetate (IDA), glycine, and glyoxylate, were included; however, the experimental results indicate rapid and complete mineralization of NTA with no build-up of soluble intermediates. The aqueous complexes and their relevant equilibrium constants (20) were taken from Stumm and Morgan (43) following Morel and Hering (56) and Martell and Smith (57, 58) and are given in Table 1. These sources provide values that are in good agreement with the recently updated National Institute of Standards and Technology (NIST) critically reviewed database of equilibrium constants except that the NIST database includes an additional Al/NTA species—a dimer (AlOHNTA)<sub>2</sub> and does not include Al(NTA)<sub>2</sub> as a potential aqueous species. For consistency with our previous work, speciation reported here (see Table 3) does not include either of these species. Their inclusion does not significantly affect the speciation (results not shown).

The dual Monod formulation (59) is used to model kinetically controlled biological reactions in CCBATCH. The rate of substrate utilization is described by  $q_{\max}$ , the maximum specific rate of substrate utilization for the bacterial species (M<sub>s</sub>M<sub>x</sub><sup>-1</sup> T<sup>-1</sup>);  $K_s$ , the half-maximum-rate concentration for the electron-donor substrate (M<sub>s</sub>L<sup>-3</sup>); and  $K_A$ , the half-maximum-rate concentration for the electron-acceptor substrate (M<sub>a</sub>L<sup>-3</sup>).  $q_{\max}$  represents the maximum capacity of the bacterial species for the utilization of this substrate, while  $K_s$  and  $K_A$  represent the affinity of the organism for the electron-donor substrate and electron-acceptor substrate, respectively. The dual Monod model predicts the rate of substrate utilization as

$$r_{\text{util}} = -q_{\max} X_a \frac{S}{S + K_s} \frac{A}{A + K_A} \quad (2)$$

in which  $X_a$  is the concentration of metabolically active organisms in the system (M<sub>x</sub>L<sup>-3</sup>),  $S$  is the available concentration of the electron-donor substrate (M<sub>s</sub>L<sup>-3</sup>),  $A$  is the concentration of the electron-acceptor substrate (M<sub>a</sub>L<sup>-3</sup>), and  $r_{\text{util}}$  is the rate of utilization of the electron-donor substrate (M<sub>s</sub>L<sup>-3</sup> T<sup>-1</sup>).

The biological utilization rate predicted by eq 2 depends on the kinetic constants as well as the concentration of the degradable form of NTA. Specific kinetic parameters have been measured for a variety of NTA degraders and NTA degradation enzymes (5–11, 17, 33, 35, 39, 60–62). VanBriesen (20) determined suitable kinetic parameters for growth of *C. heintzii* on NTA in the system studied by Bolton et al. (19) through the analysis of an independent experiment that involved the degradation of C-14 labeled NTA in the absence of complexing metals. Thus, the kinetic parameters determined by VanBriesen (20) and given in Table 2 were not determined from the experimental results analyzed here.

The biologically available form of the substrate plays a key role in the solution of eq 2. The substrate concentration,  $S$ , that controls the rate of utilization represents the concentration of the biologically available form only. Thus, the utilization rate is computed based on the concentration of the substrate available to the degrading organisms. This rate then affects the *total* concentration of substrate. The rate of substrate utilization is coupled to the stoichiometry of the degradation reaction to determine the rates of change of all the *other* components affected by the biological reaction: biomass, degradation intermediates, acidic hydrogen, in-

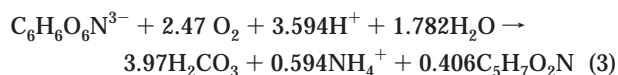
**TABLE 1. Complexes and Equilibrium Constants for NTA/Metal/*Chelatobacter heintzii* System**

complex	log β	complex	log β	complex	log β	complex	log β
H <sub>3</sub> NTA	14.38	CdOH <sup>+</sup>	-10.19	CoNH <sub>3</sub> <sup>2+</sup>	-7.325	FeNTA <sup>o</sup>	17.1
H <sub>2</sub> NTA <sup>-</sup>	12.83	Cd(OH) <sub>2</sub> <sup>o</sup>	-20.49	Co(NH <sub>3</sub> ) <sub>2</sub> <sup>2+</sup>	-15.15	Fe(NTA) <sub>2</sub> <sup>3-</sup>	25.5
HNTA <sup>2-</sup>	10.07	CuOH <sup>+</sup>	-7.79	Co(NH <sub>3</sub> ) <sub>3</sub> <sup>2+</sup>	-23.58	FeOHNTA <sup>-</sup>	12.9
OH <sup>-</sup>	13.91	Cu(OH) <sub>2</sub> <sup>o</sup>	-16.29	Co(NH <sub>3</sub> ) <sub>4</sub> <sup>2+</sup>	-32.3	Fe(OH) <sub>2</sub> NTA <sup>2-</sup>	3.9
HCO <sub>3</sub> <sup>-</sup>	-6.26	Cu(OH) <sub>4</sub> <sup>2-</sup>	-39.2	CuNH <sub>3</sub> <sup>2+</sup>	-5.33	AlNTA <sup>o</sup>	122.6
CO <sub>3</sub> <sup>2-</sup>	-16.41	Cu <sub>2</sub> (OH) <sub>2</sub> <sup>2+</sup>	-10.39	Cu(NH <sub>3</sub> ) <sub>2</sub> <sup>2+</sup>	-11.15	AlOHNTA <sup>-</sup>	7.39
NH <sub>3</sub>	-9.28	MgOH <sup>+</sup>	-11.53	Cu(NH <sub>3</sub> ) <sub>3</sub> <sup>2+</sup>	-17.68	AlHNTA <sup>+</sup>	15.3
CaCO <sub>3</sub>	-13.57	Mg <sub>4</sub> (OH) <sub>4</sub> <sup>4+</sup>	-39.54	Cu(NH <sub>3</sub> ) <sub>4</sub> <sup>2+</sup>	-25.50	Al(OH) <sub>2</sub> NTA <sup>2-</sup>	-0.89
CaHCO <sub>3</sub> <sup>+</sup>	-5.23	NiOH <sup>+</sup>	-9.99	CdNH <sub>3</sub> <sup>2+</sup>	-6.73	CaNTA <sup>-</sup>	7.06
CuCO <sub>3</sub> <sup>o</sup>	-10.07	Ni(OH) <sub>2</sub> <sup>o</sup>	-19.09	Cd(NH <sub>3</sub> ) <sub>2</sub> <sup>2+</sup>	-14.05	CdNTA <sup>-</sup>	-10.56
MgCO <sub>3</sub> <sup>o</sup>	-13.37	Ni(OH) <sub>3</sub> <sup>-</sup>	-30.0	Cd(NH <sub>3</sub> ) <sub>3</sub> <sup>2+</sup>	-22.08	Cd(NTA) <sub>2</sub> <sup>4-</sup>	14.85
MgHCO <sub>3</sub> <sup>+</sup>	-5.28	FeOH <sup>2+</sup>	-2.37	Cd(NH <sub>3</sub> ) <sub>4</sub> <sup>2+</sup>	-30.6	CdOHNTA <sup>2-</sup>	-0.95
Cu(CO <sub>3</sub> ) <sub>2</sub> <sup>2-</sup>	-23.11	Fe(OH) <sub>2</sub> <sup>+</sup>	-5.96	NiNH <sub>3</sub> <sup>2+</sup>	-6.63	CoNTA <sup>-</sup>	11.16
AlOH <sup>2+</sup>	-5.17	Fe(OH) <sub>3</sub> <sup>o</sup>	-13.32	Ni(NH <sub>3</sub> ) <sub>2</sub> <sup>2+</sup>	-13.75	Co(NTA) <sub>2</sub> <sup>4-</sup>	14.75
Al(OH) <sub>2</sub> <sup>+</sup>	-9.56	Fe(OH) <sub>4</sub> <sup>-</sup>	-21.77	Ni(NH <sub>3</sub> ) <sub>3</sub> <sup>2+</sup>	-21.38	CoOHNTA <sup>2-</sup>	0.15
Al(OH) <sub>3</sub> <sup>o</sup>	-15.26	Fe <sub>2</sub> (OH) <sub>2</sub> <sup>4+</sup>	-2.98	Ni(NH <sub>3</sub> ) <sub>4</sub> <sup>2+</sup>	-29.6	CuNTA	13.66
Al(OH) <sub>4</sub> <sup>-</sup>	-23.17	Fe <sub>3</sub> (OH) <sub>4</sub> <sup>-</sup>	-6.25	Ni(NH <sub>3</sub> ) <sub>5</sub> <sup>2+</sup>	-38.33	Cu(NTA) <sub>2</sub> <sup>4-</sup>	17.85
Al <sub>3</sub> (OH) <sub>4</sub> <sup>5+</sup>	-12.15	ZnOH <sup>+</sup>	-9.09	ZnNH <sub>3</sub> <sup>2+</sup>	-7.13	CuOHNTA <sup>4-</sup>	4.25
CaOH <sup>+</sup>	-12.94	Zn(OH) <sub>2</sub> <sup>o</sup>	-16.99	Zn(NH <sub>3</sub> ) <sub>2</sub> <sup>2+</sup>	-14.15	CuHNTA <sup>o</sup>	15.8
CoOH <sup>+</sup>	-9.73	Zn(OH) <sub>3</sub> <sup>-</sup>	-28.4	Zn(NH <sub>3</sub> ) <sub>3</sub> <sup>2+</sup>	-21.08	MgNTA <sup>-</sup>	5.96
Co(OH) <sub>2</sub> <sup>o</sup>	-18.89	Zn(OH) <sub>4</sub> <sup>2-</sup>	-41.02	Zn(NH <sub>3</sub> ) <sub>4</sub> <sup>2+</sup>	-28.4	NiNTA <sup>-</sup>	12.95
Co(OH) <sub>3</sub> <sup>-</sup>	-31.50	Zn(NTA) <sub>2</sub> <sup>4-</sup>	15.68	NiOHNTA <sup>2-</sup>	1.15	Ni(NTA) <sub>2</sub> <sup>4-</sup>	14.75
		ZnOHNTA <sup>2-</sup>	1.15	ZnNTA <sup>-</sup>	11.45	NiOHNTA <sup>2-</sup>	1.15

**TABLE 2. Kinetic Parameters for Growth of *Chelatobacter heintzii* on Nitrilotriacetic Acid**

parameter	value	units
maximum specific rate of substrate utilization for NTA ( <i>q<sub>max</sub></i> )	0.45	mol NTA mol cells <sup>-1</sup> h <sup>-1</sup>
Monod half-maximum rate constant for NTA ( <i>K<sub>s</sub></i> )	3 × 10 <sup>-6</sup>	mol NTA L <sup>-1</sup>
Monod half-maximum rate for oxygen (measured in NTA system) ( <i>K<sub>A</sub></i> )	7.81 × 10 <sup>-6</sup>	mol L <sup>-1</sup>
decay constant, <i>b</i>	4.88 × 10 <sup>-2</sup>	h <sup>-1</sup>

organic carbon, and ammonium. The biodegradation routine in CCBATCH computes a rate for each component in the degradation reaction and returns a change to the total concentration of the component for each time-step. The stoichiometry for the NTA system has been discussed previously (20, 30, 31). For NTA mineralization in a single step, the stoichiometry of the overall reaction that includes cell synthesis and substrate utilization is developed by considering cell synthesis, the electron acceptor (O<sub>2</sub>), and the electron-donor (NTA). The half reactions and thermodynamic values for these reactions are utilized to predict the coefficients for the full reaction consuming NTA and generating cells (25, 26, 31). The predicted degradation reaction based upon mineralization of NTA in a single step is



The importance of intermediate formation in the degradation of NTA by *C. heintzii* has been considered (20), and these intermediates are included in the modeling; however, for the experimental system analyzed here, complete mineralization is observed. Therefore, our analysis can avoid the potentially confounding influence of identifying the rate-limiting form of the *intermediates* on identification of the rate-limiting form of NTA.

Cell decay reactions are modeled in CCBATCH with stoichiometry coupled to kinetics to predict changes for all components affected by cell decay (20, 30, 63). For *C. heintzii* growing on NTA, the maintenance requirements were

determined experimentally by Bally et al. (6), and a decay constant was derived by VanBriesen (20) and is given in Table 2.

Following the adjustments to total component concentration based on the kinetic substrate utilization and cell decay, CCBATCH reequilibrates the aqueous speciation based on thermodynamic equilibrium and computes the updated concentration of all chemical species in the system.

## Results and Discussion

To ascertain the biologically available or rate-controlling form of NTA (e.g. NTA<sup>3-</sup>, CaNTA<sup>-</sup>, MgNTA<sup>-</sup>), experiments involving the presence of equimolar concentrations of potentially complexing metals with NTA (19) will be analyzed first. These experiments were designed to create systems in which the dominant metal-NTA species was different in each case, and other metal-NTA species were absent. However, due to the presence of cells and the metals released from them as well as the low concentration of the complexing substrate (5.23 μM NTA), all of the systems contained multiple NTA/metal and acid forms. The initial speciation of NTA, computed using CCBATCH, is shown in Table 3, along with initial rates (19).

The experimental results (19) are shown in Figure 1. No metal, Ca, and Mg gave the fastest degradation rate and showed a sharp release of C-14 CO<sub>2</sub>. Fe, Co, and Zn gave slower initial kinetics but reached approximately the same total C-14 CO<sub>2</sub> release by 15 h. Al was still slower, and Cu and Ni were the slowest and did not reach full mineralization results in the 45 h of the experiment.

Inspecting the speciation of NTA in Table 3 eliminates many of the species as potentially controlling the rate of biodegradation. Some Me-NTA forms show almost no concentration change for the different Me/NTA treatments. For example, CuNTA<sup>-</sup> represents 0.6% of the total NTA in all cases except when Cu is added equimolar to NTA. The rate of degradation changes significantly in these other cases, while the concentration of CuNTA<sup>-</sup> remains the same; therefore, CuNTA<sup>-</sup> is not the rate-controlling form. NiNTA<sup>-</sup> and FeOHNTA<sup>-</sup> show a similar pattern of constant initial speciation across many of the Me/NTA treatments; they are not the rate-controlling form of NTA.

Concentrations of other Me/NTA forms vary for some but not all of the different Me/NTA treatments. For example, ZnNTA<sup>-</sup> is 0.1% of the total NTA for cases when no-metal,

TABLE 3. Initial Percentage Speciation of NTA for Each Metal/NTA Experiment<sup>a</sup>

species	no-metal	Ca/NTA	Mg/NTA	Co/NTA	Fe/NTA	Zn/NTA	Al/NTA	Cu/NTA	Ni/NTA
NTA <sup>3-</sup>	3.60E-5	3.58E-5	3.59E-5	3.63E-6	4.02E-7	2.5E-6	7.53E-6	1.23E-7	3.49E-7
HNTA <sup>2-</sup>	92.91	92.54	92.93	9.37	1.038	6.46	19.50	3.17E-1	9.02E-1
AlNTA <sup>o</sup>	7.50E-1	7.50E-1	7.5E-1	4.7E-1	1.09E-1	3.98E-1	10.98	3.69E-2	9.67E-2
AIOHNTA <sup>-</sup>	4.63	4.6	14.63	2.91	6.75E-1	2.45	67.69	2.28E-1	5.97E-1
CaNTA <sup>-</sup>	9.75E-2	5.68E-1	9.79E-2	9.92E-3	1.10E-3	6.85E-3	2.07E-2	3.35E-4	9.52E-4
CoNTA <sup>-</sup>	5.26E-1	5.26E-1	5.26E-1	86.2	2.14E-1	4.32E-1	4.95E-1	9.06E-2	1.97E-1
CuNTA <sup>-</sup>	6.12E-1	6.12E-1	6.12E-1	6.12E-1	6.08E-1	6.12E-1	6.12E-1	99.04	6.08E-1
FeOHNTA <sup>-</sup>	1.37E-1	1.37E-1	1.37E-1	1.37E-1	95.60	1.37E-1	1.37E-1	1.25E-1	1.33E-1
MgNTA <sup>-</sup>	4.78E-3	4.76E-3	4.24E-2	4.82E-4	5.35E-5	3.33E-4	1.0E-3	1.63E-5	4.65E-5
NiNTA <sup>-</sup>	1.34E-1	1.34E-1	1.34E-1	1.33E-1	1.31E-1	1.33E-1	1.34E-1	1.24E-1	97.32
ZnNTA <sup>-</sup>	1.14E-1	1.14E-1	1.14E-1	1.06E-1	6.56E-2	89.29	1.10E-1	3.31E-2	6.16E-2
first-order rate constant	0.67a	0.75a	0.58a	0.26b	0.214b	0.19b	0.12c	0.11c,d	0.063d

<sup>a</sup> Numbers in the last row followed by the same letter are not significantly different at the 95% confidence interval (19).

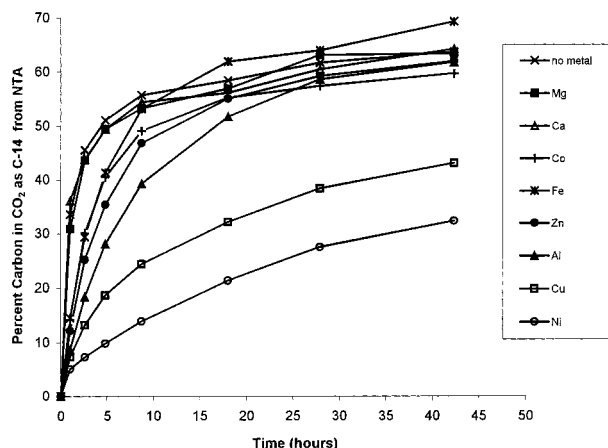


FIGURE 1. Experimental results for <sup>14</sup>CO<sub>2</sub> release curves in various metal/NTA systems. Initial speciation of the various metal/NTA systems is shown in Table 3.

Ca, Mg, Co, or Al are added equimolar with NTA. These five cases show significantly different rates; therefore, modeling based on ZnNTA<sup>-</sup> as the bioavailable, degradable form will not capture the experimental observations.

Other Me-NTA concentrations (AlNTA<sup>o</sup>, AIOHNTA<sup>-</sup>, CoNTA<sup>-</sup>) vary in the different treatments but show no systematic relationship to the degradation rates. Furthermore, none of the treatments in which the Me/NTA form is dominant shows a degradation rate as rapid as the no-metal case. If a metal-NTA form were the actively degraded form of the chelate, we would expect the initial rate of degradation to be more rapid when that form has the highest concentration (a larger percentage of the total NTA). A possible exception would be if a metal/NTA form was degraded utilizing a transport system that is saturated at very low concentrations of the degradable form. For example, if AIOHNTA<sup>-</sup> were the degradable form and its transport saturation concentration was less than the  $2.4 \times 10^{-7}$  M (4.6% of 5.23  $\mu$ M) present in the no-metal, Ca, and Mg systems, then the rate with higher concentrations of AIOHNTA<sup>-</sup> (67.7% in the Al/NTA trial) would not be higher. However, the saturated rate in the Al/NTA trial should be as high as in the no-metal case. However, that result is not observed for AIOHNTA<sup>-</sup> or the other two complexes (AlNTA<sup>o</sup>, CoNTA<sup>-</sup>).

For CaNTA<sup>-</sup> and MgNTA<sup>-</sup>, however, rates in equimolar systems are approximately as fast as the rate in the no-metal system, and these forms could be the rate-controlling degradable substrate form. Further, the most rapid rates (no metal, Ca, and Mg) occur in systems that have the highest concentrations of CaNTA<sup>-</sup> and MgNTA<sup>-</sup>. The slowest rates

(the Cu and Ni treatments) occur in systems that have the lowest concentrations of these forms. The acid forms, NTA<sup>3-</sup> and HNTA<sup>2-</sup>, also show good agreement between relative speciation and initial degradation rate. The most rapid degradation occurs in systems with the highest initial concentration of HNTA<sup>2-</sup> and NTA<sup>3-</sup> (the no-metal, Ca, and Mg treatments), and slowest degradation occurs in systems with the lowest initial concentration of these forms. A discrepancy is observed in the Al/NTA case, where the concentration of HNTA<sup>2-</sup>, NTA<sup>3-</sup>, CaNTA<sup>-</sup>, and/or MgNTA<sup>-</sup> are an order of magnitude higher than in the Cu/NTA case, but the initial rates are not significantly different. As mentioned previously, different sources report different species that form in solution from Al and NTA. These differences may account for the rate observed in the Al/NTA case.

Based on these analyses, we conclude that the biologically available, rate-controlling form(s) must be HNTA<sup>2-</sup>, NTA<sup>3-</sup>, CaNTA<sup>-</sup>, and/or MgNTA<sup>-</sup>. However, the Me/NTA data are not sufficient to distinguish which of these forms are biologically available, because the concentration changes to each of these forms between the treatments follow the same pattern. For example, the no-metal case and the Ni/NTA case give the fastest and slowest rates, respectively, which differ approximately 100-fold. Likewise, the concentration of HNTA<sup>2-</sup>, NTA<sup>3-</sup>, CaNTA<sup>-</sup>, and MgNTA<sup>-</sup> differ approximately 100-fold between these two experiments (Table 3).

Due to the same pattern of changes in concentration, we can accurately model these systems with the assumption that any one of these four forms is the rate-limiting form by adjusting the half-maximum rate constant concentration ( $K_s$ ) for the four cases. Figure 2 shows model predictions (the solid lines that are nearly coincidental) based on each of the four potentially rate-limiting forms and four different half-maximum rate constants for the no-metal, Co/NTA, and Ni/NTA cases. The  $K_s$  values used for these predictions are estimated based on the literature reported  $K_s$  value (39, 64) of  $3 \times 10^{-6}$  M and an adjustment based on the relative concentration of the proposed rate-limiting form. For example, since the concentration of NTA<sup>3-</sup> is approximately 4 orders of magnitude lower than HNTA<sup>2-</sup> at pH 6, the  $K_s$  value used for the model with NTA<sup>3-</sup> as rate-limiting is  $10^{-10}$  M, while the  $K_s$  value for the model based on HNTA<sup>2-</sup> is  $10^{-6}$  M.

The  $K_s$  value for HNTA<sup>2-</sup> utilized for Figure 2 is approximately equivalent to the literature-reported values (39, 64) and the value determined by VanBriesen (20). We might conclude that NTA<sup>3-</sup>, CaNTA<sup>-</sup>, and MgNTA<sup>-</sup> are not rate-limiting degradable forms because of the very low  $K_s$  values required to produce predictive model results. However, the literature values for  $K_s$  represent concentrations based on total concentration of NTA, and the value utilized in modeling

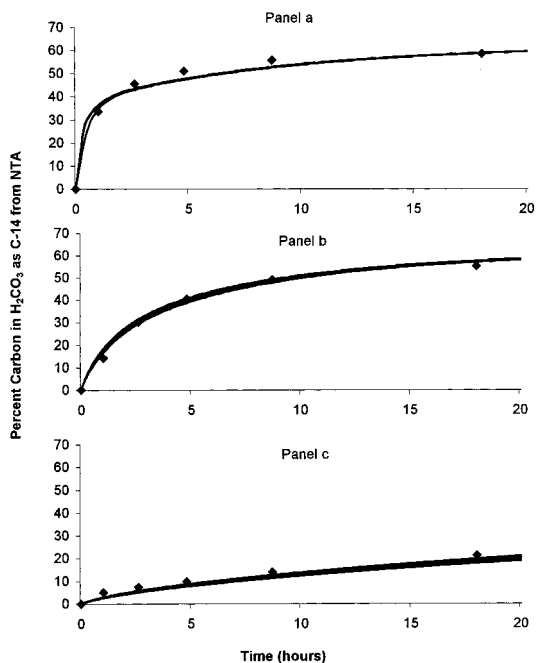


FIGURE 2. Model and experimental results in no-metal (panel a), Co/NTA (panel b), and Ni/NTA (panel c) systems. Model trials shown are based on four different degradable forms.

TABLE 4. Initial Percentage Speciation for NTA Degradation at Different pHs

species	pH 6	pH 7	pH 8
NTA <sup>3-</sup>	7.91E-3	7.98E-2	7.67E-1
HNTA <sup>2-</sup>	92.9	93.7	90.10
CaNTA <sup>-</sup>	9.79E-2	9.47E-1	6.51
MgNTA <sup>-</sup>	1.34E-1	1.34E-1	1.34E-1

biodegradation following dual Monod kinetics (eq 2) must be the value based on the concentration of the *biologically available, rate-controlling form*. Details of the metals in solution with the NTA when the half-maximum concentration was measured are not reported (64); however, since cells must have been present, we can assume some Ca and Mg from cell walls would have been available for complexation. CaNTA<sup>-</sup> and MgNTA<sup>-</sup> would have represented some fraction of the NTA available to the cells, and the  $K_s$  for these degradable species would be some fraction of the  $K_s$  reported based on the total concentration of NTA. Therefore, without additional details of the conditions under which  $K_s$  was measured, we cannot rule out the possibility that CaNTA<sup>-</sup>, MgNTA<sup>-</sup>, or NTA<sup>3-</sup> was the rate-controlling form, despite the very low concentrations of these forms in the experimental system and the correspondingly low  $K_s$  values required for predictive modeling.

To narrow the possible rate-controlling form, we consider the second set of experiments (48) on NTA biodegradation. In these experiments, the degradation of 1  $\mu$ M NTA in the absence of metals at pH 6, 7, and 8 produces speciation changes to the four possible rate-controlling forms of NTA that are different. Speciation for the relevant complexes under these conditions is shown in Table 4, and the experimental results for CO<sub>2</sub> release are shown in Figure 3 along with model predictions. The experimental results show an obvious pH effect, with degradation fastest at pH 8 (complete by about 2 h; panel c) and significantly slower at pH 6 (incomplete by 10 h; panel a). The speciation results indicate that the dominant NTA form across all pHs is HNTA<sup>2-</sup> (90–93.7%) and MgNTA<sup>-</sup> remains approximately 0.13% in all cases. On the other hand, the fraction contained in NTA<sup>3-</sup> and CaNTA<sup>-</sup>

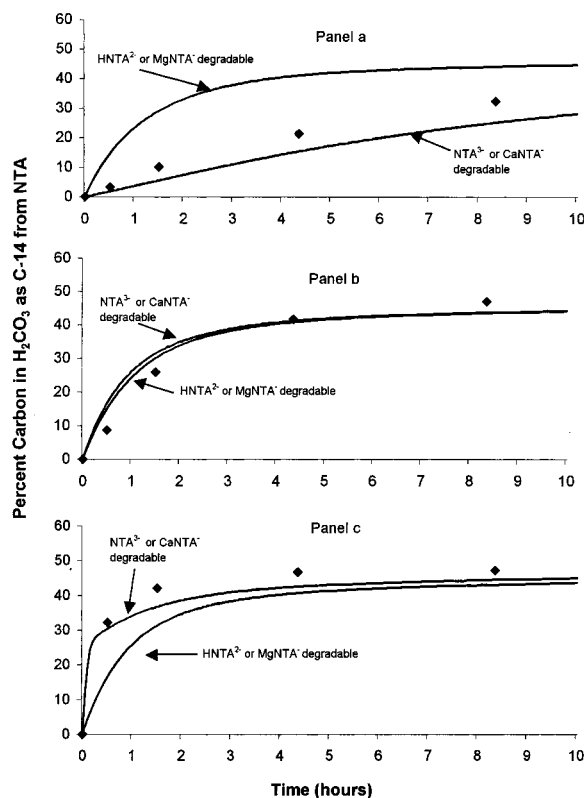


FIGURE 3. Experimental and model results for NTA degradation at different pHs. Panel a is pH 6, panel b is pH 7, and panel c is pH 8.

increases almost 10-fold with each pH unit. Thus, we would expect that, if NTA<sup>3-</sup> or CaNTA<sup>-</sup> were the rate controlling form, the rate of degradation should be faster at pH 8 than at pH 6. On the other hand, the difference would be small if HNTA<sup>2-</sup> or MgNTA<sup>-</sup> were the degradable form. Model results using each of the possible forms as rate-controlling for NTA degradation, shown in Figure 3, confirm that NTA<sup>3-</sup> and CaNTA<sup>-</sup> gave the observed response to pH, while HNTA<sup>2-</sup> and MgNTA<sup>-</sup> did not predict the data.

None of the experiments described thus far (19, 48) provide a chemical system that could be used to differentiate between NTA<sup>3-</sup> or CaNTA<sup>-</sup> as potential rate controlling, degradable forms. The most reasonable experimental system for this determination would be a set of experiments with different NTA to Ca ratios. Therefore, two additional experiments were conducted, following the same procedures as described above. In the first, equimolar Ca and NTA at 1  $\mu$ M was considered. In the second, the calcium concentration was significantly in excess of NTA (Ca at 10 mM and NTA at 1  $\mu$ M). Under these conditions, the initial NTA speciation for the two systems is very different. At pH 7 in the equimolar case, the distribution of major species predicted at thermodynamic equilibrium is as follows: 85% HNTA<sup>2-</sup>, 6% AlOHNTA<sup>-</sup>, 3% CuNTA<sup>-</sup>, and 3% CoNTA<sup>-</sup>. NTA<sup>3-</sup> is 0.08% and CaNTA<sup>-</sup> is 0.9%. For the case with a calcium concentration of 10 mM, the distribution of major species is as follows: 93% CaNTA<sup>-</sup>, 3% CuNTA<sup>-</sup>, and 1.5% CoNTA<sup>-</sup>. NTA<sup>3-</sup> makes up less than 0.0008% of the NTA. Figure 4 shows model simulations and experimental results (panel a shows the equimolar case while panel b shows the case of excess Ca). Clearly, the different relative concentrations of CaNTA<sup>-</sup> and NTA<sup>3-</sup> for these two experimental systems result in different predictions of CO<sub>2</sub> release. Modeling based on CaNTA<sup>-</sup> as the rate-limiting, biologically available form is predictive for NTA degradation by *C. heintzii*.

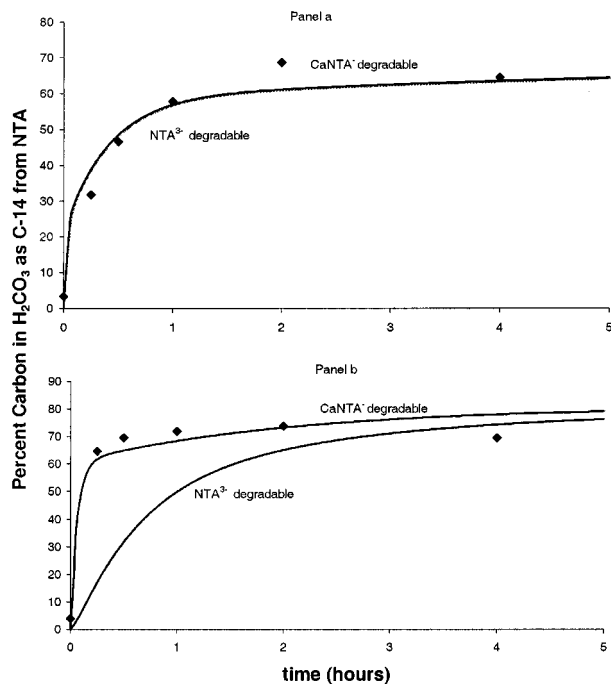


FIGURE 4. Model prediction and experimental results of  $\text{CO}_2$  release from different Ca:NTA systems with different assumed degradable form. Panel a is for equimolar NTA and Ca at  $1 \mu\text{M}$ . Panel b is for NTA at  $1 \mu\text{M}$  and Ca and  $10 \text{mM}$ .

From these analyses, we see that a single aqueous form ( $\text{CaNTA}^-$ ) can be used to describe degradation of NTA in Me/NTA systems without consideration of metal-complexation kinetics. Since this chemical species is not dominant in aqueous solution under the experimental conditions, its formation from the dominant Me-NTA or  $\text{HNTA}^{2-}$  species in aqueous solution must have been rapid. We conclude complexation exchange kinetics in the bulk solution probably are not rate-limiting. Complexation exchange kinetics inside the cell probably are also not rate-limiting. The  $\text{CaNTA}^-$  is not a substrate for NTA monooxygenase (NTA-MO), the first degradative enzyme (13, 42). However,  $\text{MgNTA}^-$  is a substrate for NTA-MO (13, 42) and given the micromolar concentrations of Mg in microbial cytoplasm (65) the exchange of  $\text{Mg}^{2+}$  for the  $\text{Ca}^{2+}$  to form  $\text{MgNTA}^-$  in the cytoplasm must also be rapid. Thus, the rate-controlling step for NTA degradation appears to be the transport of the  $\text{CaNTA}^-$  form into the cell.

The presence of  $1 \text{mM}$  Ca significantly enhanced the rate of NTA transport into *C. heintzii*, with the maximum rate obtained at  $1 \mu\text{M}$  concentration of NTA (Figure 5). A saturation curve was found for cells grown on NTA or acetate, with the transport rate much higher for NTA grown cells. The enhanced transport of  $\text{CaNTA}^-$  in acetate grown cells suggests a constitutive level of transport protein is expressed. The transport of NTA without Ca for both NTA and acetate grown cells did not display a saturation curve but rather a linear curve suggesting diffusion rather than active transport. Inhibitors of ATP generation including CCCP ( $50 \mu\text{M}$ ), sodium azide ( $10^{-2} \text{M}$ ), and 2,4-dinitrophenol ( $10^{-3} \text{M}$ ) all inhibited the transport of  $1 \mu\text{M}$  CaNTA at 1.2%, 1.7%, and 1.0% of the control respectively, suggesting that ATP generation is essential for the active transport of  $\text{CaNTA}^-$ .

There was a similar rate of transport for C-14 NTA and  $^{45}\text{Ca}$  into *C. heintzii* up to a concentration of  $0.5 \mu\text{M}$  CaNTA $^-$ , with some divergence at  $0.75 \mu\text{M}$  and a parallel rate after this (Figure 6). The equal molar transport of both Ca and NTA demonstrate that the  $\text{CaNTA}^-$  complex is the species transported into the cell and the rate-controlling substrate.

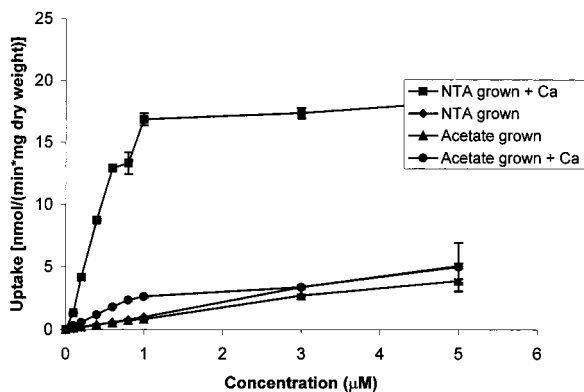


FIGURE 5. Transport rate of varying concentrations of NTA with and without  $1 \text{mM}$  Ca at pH 7 in *C. heintzii* when grown on NTA or acetate.

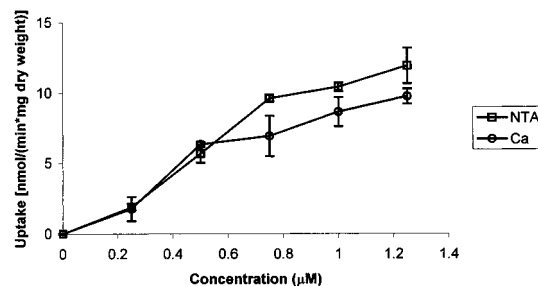


FIGURE 6. Transport rate of either  $^{14}\text{C}$ -NTA or  $^{45}\text{Ca}$  as a function of CaNTA concentration in *C. heintzii* at pH 7.

This work represents a significant contribution to understanding chelate biotransformation in environmental systems. We present the first identification of a specific rate-controlling aqueous chelate form in the degradation of NTA by *C. heintzii*. Accelerated biotreatment of NTA wastes could be accomplished by changes to the aqueous speciation that increase the  $\text{CaNTA}^-$  form in solution. The potential for intrinsic or enhanced bioremediation could be assessed by an evaluation of the natural mineral composition at the site and the likelihood of high concentrations of the rate-limiting form. Additional research in identification of the rate-limiting form in systems that include more recalcitrant chelating agents (e.g., ethylenediaminetetraacetate (EDTA)) could lead to new methods for evaluating and enhancing bioremediation of these contaminants.

## Acknowledgments

This research was funded by the Office of Biological and Environmental Research, U.S. Department of Energy's Subsurface Science Program and Natural and Accelerated Bioremediation Research Program. The continued support of Dr. Frank Wobber and Dr. Anna Palmisano is gratefully acknowledged.

## Literature Cited

- (1) Ayres, J. A. *Decontamination of Nuclear Reactors and Equipment*; Ronald Press: New York, 1970.
- (2) Piciulo, P. L.; Adams, J. W.; David, M. S.; Milian, L. W.; Anderson, C. I. *Release of Organic Chelating Agents From Solidified Decontamination Wastes*; National Technical Information Service: Springfield, VA, 1986.
- (3) McFadden, K. M. *Organic Components of Nuclear Wastes and Their Potential for Altering Radionuclide Distribution When Released to Soil*; National Technical Information Service: Springfield, VA, 1980.
- (4) Baik, M. H.; Lee, K. J. *Ann Nucl Energy* **1994**, *21*(2), 81–96.
- (5) Auling, G.; Busse, H.-J.; Egli, T.; El-Banna, T.; Stackebrandt, E. *Systematic Appl. Microbiol.* **1993**, *16*, 104–112.

- (6) Bally, M.; Wilberg, E.; Kuhni, M.; Egli, T. *Microbiology* **1994**, *140*, 1927–1936.
- (7) Bally, M.; Egli, T. *Appl. Environ. Microbiol.* **1996**, *62*(1), 133–140.
- (8) Egli, T.; Bally, M.; Uetz, T. *Biodegradation* **1990**, *1*, 121–132.
- (9) Egli, T. *Experientia* **1990**, 404–406.
- (10) Egli, T. *Biochemistry of Microbial Degradation*; Ratledge, C., Ed.; Kluwer Academic Publishers: New York, 1994; pp 179–195.
- (11) Uetz, T.; Schneider, R.; Snozzi, M.; Egli, T. *J. Bacteriol.* **1992**, *174*(4), 1179–1188.
- (12) Gudernatsch, H. *Gas U-WassFach* **1975**, *116*, 512–517.
- (13) Huber, W.; Popp, K. H. *Fette Seife Anst* **1972**, *74*, 166–8.
- (14) Chau, Y. K.; Shiomu, M. T. *Water, Air, Soil Pollut.* **1972**, *1*, 149–164.
- (15) Swisher, R. D.; Taulli, T. A.; Malec, E. J. *Trace Metals and Metal Organic Interactions in Natural Waters*; Singer, P. C., Ed.; Ann Arbor Science Publishers: Ann Arbor, MI, 1973; pp 237–263.
- (16) Tiedje, J. M.; Mason, B. B. *Proc. Soil Sci. Soc. Am.* **1974**, *38*, 278–283.
- (17) Firestone, M. K.; Tiedje, J. M. *Appl. Microbiol.* **1975**, *29*, 758–64.
- (18) Madsen, E. L.; Alexander, M. *Appl. Environ. Microbiol.* **1985**, *50*(2), 342–349.
- (19) Bolton, H. Jr.; Girvin, D. C.; Plymale, A. E.; Harvey, S. D.; Workman, D. J. *Environ. Sci. Technol.* **1996**, *30*(3), 931–938.
- (20) VanBriesen, J. M. Ph.D. Dissertation, Northwestern University, Evanston, IL, 1998.
- (21) Bolton, H. Jr.; Li, S. W.; Workman, D. J.; Girvin, D. C. *J. Environ. Quality* **1993**, *22*, 125–132.
- (22) McCarty, P. L. *The Fifth Rudolf Research Conference*; 1969.
- (23) McCarty, P. L. *Organic Compounds in Aquatic Environments*; Faust, S. D. a. H. J. V., Ed.; Marcel Dekker: New York, 1971.
- (24) McCarty, P. L. *Water Pollution Microbiology*; Mitchell, R., Ed.; Wiley-Interscience: New York, 1972.
- (25) McCarty, P. L. *Paper Presented at the International Conference Toward a Unified Concept of Biological Waste Treatment Design*; 1972.
- (26) McCarty, P. L. *Prog. Water Technol.* **1975**, *7*, 157–172.
- (27) Christensen, D. R.; McCarty, P. L. *J. Water Pollut. Control Federation* **1975**, *47*(11), 2652–2664.
- (28) Lawrence, A. W.; McCarty, P. L. *ASCE J. Sanitary Engineering Division* **1970**, *96*(nSA3), 757–778.
- (29) Metcalf, Eddy, I. *Wastewater Engineering: Treatment, Disposal, and Reuse*; McGraw-Hill Inc.: New York, 1991.
- (30) Rittmann, B. E.; VanBriesen, J. M. *Reviews in Mineralogy, Vol 34: Reactive Transport in Porous Media*; Lichtner, P. C., Steefel, C. I., Oelkers, E. H., Eds.; Mineralogical Society of America: 1996; p 311.
- (31) VanBriesen, J. M.; Rittmann, B. E. *Biotechnol. Bioeng.* **2000**, *67*(1), 35–52.
- (32) Egli, T. *Microbiological Sci.* **1988**, *5*(2), 36–41.
- (33) Egli, T.; Weilenmann, H.-U.; El-Banna, T.; Auling, G. *System Appl. Microbiol.* **1988**, *10*, 297–305.
- (34) Tiedje, J. M.; Firestone, M. K.; Mason, B. B.; Warren, C. B. *Abstracts of the Annual Meeting of Microbiologists*; 1973; p 171.
- (35) Firestone, M. K.; Tiedje, J. M. *Appl. Environ. Microbiol.* **1978**, *35*, 955–961.
- (36) Xu, Y.; Mortimer, M. W.; Fisher, T. S.; Kahn, M. L.; Brockman, F. J.; Xun, L. *J. Bacteriol.* **1997**, *179*(4), 1112–1116.
- (37) Jenal-Wanner, U. Ph.D. Thesis, Swiss Federal Institute of Technology, Zurich, Switzerland, 1991.
- (38) Xun, L.; Reeder, R. B.; Plymale, A. E.; Girvin, D. C.; Bolton, H. Jr. *Environ. Sci. Technol.* **1996**, *30*, 1752–1755.
- (39) Alder, A. C.; Siegrist, H.; Gujer, W.; Giger, W. *Water Res.* **1990**, *24*(6), 733–742.
- (40) Wilberg, E.; El-Banna, T.; Auling, G.; Egli, T. *Systematic Appl. Microbiol.* **1993**, *16*, 147–152.
- (41) Wilberg, E. Zurich, Switzerland, 1989.
- (42) Morel, F.; Morgan, J. *Environ. Sci. Technol.* **1972**, *6*(1), 58–67.
- (43) Stumm, W.; Morgan, J. J. *Aquatic Chemistry*, 3rd ed. Wiley-Interscience: New York, 1996.
- (44) Sigg, L.; Xue, H. *Chemistry of Aquatic Systems: Local and Global Perspectives*; Bidoglio, G., Stumm, W., Eds.; ECSC, EEC, EAEC: The Netherlands, 1994; pp 153–181.
- (45) Xue, H.; Sigg, L.; Kau, F. G. *Environ. Sci. Technol.* **1995**, *29*, 59–68.
- (46) Nowack, B.; Xue, H.; Sigg, L. *Environ. Sci. Technol.* **1997**, *31*, 866–872.
- (47) Wong, P. T. S.; Liu, D.; Dutka, B. J. *Water Res.* **1972**, *6*, 1577–1584.
- (48) Bolton, H. Jr.; Girvin, D. C. *Environ. Sci. Technol.* **1996**, *30*, 2057–2065.
- (49) Good, N. E.; Winget, G. D.; Winter, W.; Connolly, T. N. *Biochemistry* **1966**, *5*, 467–477.
- (50) Jardim, W. F.; Allen, H. E. *The Kinetics of Trace Metal Complexation: Implications for Metal Reactivity in Natural Waters*; Kramer, C. J. M., Duinker, J. C., Eds.; John Wiley and Sons: New York, 1984; pp 145–172.
- (51) Lichtner, P. C. *Geochem. Cosmochim. Acta* **1985**, *49*, 779–800.
- (52) Yeh, G. T.; Tripathi, V. S. *Water Resources Res.* **1989**, *25*(1), 93–108.
- (53) Engesgaard, P.; Kipp, K. K. *Water Resources Res.* **1992**, *28*(10), 2829–2843.
- (54) Lichtner, P. C. *Reviews in Mineralogy, Vol 34: Reactive Transport in Porous Media*; Lichtner, P. C. S. C. I. O. E. H., Editors; Mineralogical Society of America: 1996; pp 1–81.
- (55) McCarty, P. L. *Advances in Water Pollution Research: Proceedings of the 2nd International Conference on Water Pollution Research*; Baers, J., Ed.; Pergamon Press: Oxford, England, 1965; Vol. 2, pp 169–199.
- (56) Morel, F. M. M.; Hering, J. G. *Principles and Applications of Aquatic Chemistry*; John Wiley and Sons: New York, 1993.
- (57) Martell, A. E.; Smith, R. M. *Critical Stability Constants: Volume 5 First Supplement*; Plenum Press: New York, 1982.
- (58) Martell, A. E.; Smith, R. M. *Critical Stability Constants: Volume 1 Amino Acids*; Plenum Press: New York, 1982.
- (59) Bae, W.; Rittmann, B. E. *Biotechnol. Bioeng.* **1996**, *49*, 683–689.
- (60) Egli, T.; Weilenmann, H.-U. *Toxicity Assessment: Int. J.* **1989**, *4*, 23–34.
- (61) Wong, P. T. S.; Liu, D.; McGirr, D. J. *Water Res.* **1973**, *7*, 1367–1374.
- (62) Firestone, M. K.; Aust, S. D.; Tiedje, J. M. *Archives Biochemistry Biophysics* **1978**, *190*(2), 617–623.
- (63) VanBriesen, J. M.; Rittmann, B. E. *Accepted in Biodegradation*.
- (64) Siegrist, H.; Alder, A.; Gujer, W.; Giger, W. *Water Sci. Technol.* **1989**, *21*, 315–324.
- (65) Hughes, M. N.; Poole, R. K. *Metals and Microorganisms*; Chapman and Hall: New York, 1989.

Received for review October 18, 1999. Revised manuscript received May 16, 2000. Accepted May 18, 2000.

ES991190K